An experimental/numerical hybrid methodology for the prediction of railway-induced ground-borne vibration on buildings to be constructed close to existing railway infrastructures: Numerical validation and parametric study

Robert Arcos [a,b,*], Paulo J. Soares [b], Pedro Alves Costa [b,c], Luís Godinho [d]

[a] Serra Húnter Fellow, Acoustical and Mechanical Engineering Laboratory (LEAM), Universitat Politècnica de Catalunya (UPC), Carrer Colom, 11, 08222, Terrassa (Barcelona), Spain
[b] CONSTRUCT, Faculty of Engineering (FEUP), University of Porto, Rua Dr. Roberto Frias, S/n, 4200-465, Porto, Portugal
[c] Visiting Cheney Fellow, Institute for High Speed Rail and Systems Integration, School of Civil Engineering, University of Leeds, UK
[d] ISISE, Dep. Civil Engineering, University of Coimbra. Pólo II, Rua Luís Reis Santos, 3030-788, Coimbra, Portugal

ARTICLE INFO

ABSTRACT

A novel experimental/numerical hybrid methodology for the assessment of railway-induced ground-borne vibration in buildings based on experimental measurements in the soil surface is proposed in this paper. This methodology has been specifically designed for the prediction of railway-induced vibration in buildings to be constructed close to an operative railway infrastructure, although it can be applied for other types of vibration sources. The model of the incident wave field induced by the railway infrastructure consists of a set of virtual forces applied in the soil, which would be obtained from vibration experimental measurements in the surface of the ground where the building will be constructed. These virtual forces can be subsequently applied to a model of the building-soil system to obtain a prediction of the vibration levels that will be induced by the existing railway infrastructure to the studied building. In the present work, this methodology is theoretically defined and it is numerically validated for two-dimensional and two-and-a-half-dimensional cases. To numerically test the methodology, the measured ground surface responses are replaced by simulated ones obtained in a set of points called collocation points. In this context, a parametric study has been developed with the aim of finding out a robust criterion for the application of the present methodology with respect to the amount and location of the collocation points (representing vibration sensors) and virtual forces. It is found that the distance between virtual sources should be smaller than the S-wave wavelength of the upper soil layer corresponding to the highest frequency of the frequency range of interest to ensure the reliability of the methodology. Moreover, the proposed method is found to be insignificantly affected by the building-tunnel dynamic coupling for building-tunnel distances above 20 m. The proposed hybrid model would simplify the usual numerical prediction approach commonly adopted for dealing in detail with these problems, since a model of the railway infrastructure is no longer required. Moreover, it would reduce the uncertainty of the prediction due to the use of experimental measurements of the particular site to be studied. In addition, it would provide a higher accuracy and flexibility than empirical models based on experimental transmissibility functions between the soil surface and the building.

1. Introduction

Nowadays, railway-induced noise and vibration is a public concern. Many countries all around the world have established regulations for the maximum noise and vibration levels that can be reached in buildings near a railway infrastructure. These regulations are set mainly to control the annoyance to the building inhabitants, but also to ensure the correct operation of sensitive machinery and equipment and, eventually, to avoid any building damage (usually non-structural). In particular, since most of the urban railway networks around the world are underground,

railway-induced ground-borne noise and vibration has become a highly important railway-based source of environmental pollution in urban environments.

One of the most common situations in which a railway-induced noise and vibration assessment study is required is when a new building is decided to be constructed near an existing and operational urban railway line. In such cases, the railway line administration or the city council usually demands a study that certifies that the maximum railway-induced ground-borne noise and vibration levels that will be achieved in the future building will comply with the applicable noise and vibration regulations. Thus, in those situations, prediction models of the railway-induced ground-borne noise and vibration levels inside buildings are required.

Various theoretical models that account for the comprehensive system, i.e. the railway infrastructure, the soil and the building to be studied, have been developed during last three decades. One of the first proposals in this regard was presented by Balendra et al. [1,2], who proposed a methodology that uses a two-dimensional (2D) finite element method (FEM) model to compare the train-induced vibration in a building for two tunnel track systems. Handling the problem from a different perspective, Trochides [3] proposed a simple method based on statistical energy analysis concepts for predicting ground-borne vibrations levels in buildings near to underground railway infrastructures. However, three-dimensional (3D) modelling approaches are more accurate to obtain the building response in the context of railway-induced ground-borne vibration [4]: they account for the wave propagation in the longitudinal direction and they are able to represent rigorously moving loads. Fiala et al. [5] used a decoupled 3D approach to assess the vibration response of a building. This approach considers a weak coupling between the tunnel-soil and the building-soil systems. For the tunnel-soil system, a two-and-a-half-dimensional (2.5D) FEM model for the tunnel coupled with a 2.5D boundary element method (BEM) model for the soil [6] was used in that work. For the building-soil model, a 3D FEM-BEM model was adopted. A similar approach was presented by Lopes et al. [7,8], where, in this case, the tunnel-soil system is modelled by using a 2.5D FEM with perfect matched layers (PML). In [9], Hussein et al. proposed a 3D model of the comprehensive system by using semi-analytical approaches for modelling the building and the tunnel-soil systems. In that work, the building structure, considered to be coupled to the soil by piled foundations, is modelled as a 2D frame based on axial and bending beam elements.

In engineering practice, empirical prediction models are widely used because of their simplicity and low associated engineering costs. The Federal Railroad Administration (FRA) and the Federal Transit Administration (FTA) of the U.S. Department of Transportation presented a comprehensive empirical model for the prediction of vibration levels due to railway traffic [10], which has become probably the most used of those approaches. Empirical methods can be used for scoping modelling of railway-induced ground-borne vibrations. However, the reliability of empirical methods decreases drastically when the level of detail and required accuracy of the assessment study increases, as shown recently by Sadeghi et al. [11] for the case of the FTA guidance. Their low adaptability to particular cases makes these methods specially not suitable for detailed or design studies [12]. In the particular point of view of the receiver (the building structure), Lurcock et al. [13] and, more recently, Anderson et al. [14] showed significant differences between FTA guidance and measured data for up to 8-storey and 60-storey buildings, respectively, in terms of inter-storey vibration attenuation. The limitations of the soil-building coupling loss factors proposed by the FTA has been also shown in [15]. In order to extend the applicability of empirical methods, several semi-empirical methodologies have been reported, which consider the addition of analytical expressions or numerical models to enhance the accuracy of the overall prediction. In this regard, several investigations proposed the use of a simple Rayleigh wave propagation law to model the vibration propagation in the soil [16,17]. These methods are the first steps in experimental/theoretical

hybrid modelling in railway-induced noise and vibration problems.

The uncertainty on the railway-induced ground-borne predictions in buildings due to the imperfect knowledge of the local subsoil conditions is found to be significant in various scientific works. Twenty years ago, Lombaert et al. [18] presented a study of the effect of the soil stratification on the free field traffic-induced vibrations, demonstrating a large influence of underlying and top soil layers on the low and high frequency response of the soil surface, respectively. Thus, the unavoidable uncertainty in the soil stratification profile leads to uncertain vibration predictions [19]. Later, Jones et al. [20] quantified that soil inhomogeneity could lead to levels of uncertainty of at least ±5 dB. In order to assess the uncertainty on the vibration response, probabilistic models for soil-structure interaction (SSI) problems have been developed [21,22]. Lopes et al. [23] performed a parametric study over a building/soil model also showing the significant influence of the soil condition on the building response due to its influence on the incident wave field and the building-soil dynamic coupling. Recently, Papadopoulos et al. [24] examined the building/soil interaction problem by means of a stochastic 3D FEM-PML model in which the shear modulus of the local subsoil is assumed to be a conditional random field. They concluded that, above 10 Hz, uncertain subsoil condition results in uncertain modal characteristics for the coupled building-soil system and in an uncertain incident wave field, which particularly affects the lateral and the vertical response of the building, respectively. The same research group presented an extensive measurement campaign showing clear experimental evidences of the uncertainty on the vibration response induced by the uncertainty of the soil condition [25]. In order to reduce the uncertainty of computational models, hybrid modelling based on the combination between in situ experimental data and a theoretical model is an interesting alternative [26]. In the framework of hybrid modelling for soil-building dynamic interaction problems, Auersch [27] presented a semi-empirical model that combines pre-calculated results obtained from detailed numerical models, a database of experimental data built from several experimental measurements and several specific analytical models. Sanayei et al. [28] proposed a hybrid approach where building is modelled by finite axial rods with added floor impedance obtained from infinite thin plate models, and where the incident wave field is represented by previously known column base forces or measured vibrations at the loading dock floor. More recently, López-Mendoza et al. [29] have presented a computationally efficient model based on modal superposition to predict the ground-borne railway-induced vibration levels in buildings considering SSI. The methodology is designed, specifically, for cases where the incident wave field is known, because it is previously computed numerically or because it is measured in the ground surface. This model accounts for the SSI by adding spring and damper elements to the foundation of the building model. In a very recent work, these authors present an even faster model that uses a 3D time-domain FEM approach for the structure modelling and more elaborated spring-damper elements to account for the SSI [30]. Kuo et al. [15] presented a hybrid model that combines recorded data and numerical predictions considering the definitions proposed by the FTA [10]. In that work, the source, propagation and receiver mechanisms are uncoupled.

In the present work, a new methodology for the prediction of the ground-borne vibration induced by traffic in operational urban railway lines in buildings (or other structures) to be constructed in the surroundings of these railway infrastructures is described and numerically validated. Moreover, the method has been subjected to a numerical parametric study with the aim of defining what are the working conditions of the method that result in accurate performances. The practical application of this method uses railway-induced vibrations measured in the ground where the new building will be constructed to compute a set of virtual forces that represent the incident wave field induced by the nearby operational railway line. These virtual forces are then used on a theoretical model of the particular building-soil system to be studied in order to predict the vibration levels at any point of the structure. Thus,

this method considers a weak coupling between the railway infrastructure and the building structure. This assumption was demonstrated to be valid by Coulier et al. [31] for building-tunnel distances larger than the wavelength of the soil P-wave. This hybrid method simplifies the typical numerical procedure to deal with these problems in detail, since a model of the railway infrastructure is no longer required. Moreover, it reduces the uncertainty of the prediction due to the use of experimental measurements of the particular site to be studied, making the method highly suitable for detailed studies. In this paper, the proposed method is studied numerically by using synthetic data instead of experimental measurements on the ground surface. The methodology is numerically validated for the general problem of a two-storey building with shallow foundations at the surroundings of an underground railway line modelled by 2D and 2.5D models and accounting in both cases for homogeneous and layered soils and different building locations with respect to the tunnel.

2. Methodology

In this section, the new hybrid methodology for the prediction of railway-induced ground-borne vibration in buildings to be constructed near to urban railway lines is presented. This is a hybrid method, since it combines experimental measurements on the soil surface and a numerical model of the building-soil system. The method is based on an approach similar to the method of fundamental solutions (MFS) applied to scattering and radiation problems [32]. The MFS uses a set of virtual forces, computed ensuring that they satisfy a previously known boundary condition (or set of boundary conditions), to obtain an equivalent representation of the source or the incident field. These boundary conditions are evaluated in a set of points called collocation points. Knowing the fundamental solution associated with the wave propagation in the medium due to the type of virtual forces considered (normally point loads), the response of the system at any point of the domain can be calculated. Typically, this method considers the placement of the virtual forces outside the domain and the collocation points at the boundary of the domain. For exterior problems, the domain boundary surrounds the source, while, for interior problems, surrounds the domain. This method has proved effective in elastodynamic problems, as shown in [33,34].

The methodology presented in this paper was previously introduced by Arcos et al. [35] in a preliminary study. A similar approach was also presented in [36], which weakly couples a model of a railway tunnel embedded in a homogeneous full-space with a layered half-space system. The present methodology exhibits three important differences with respect to the classical MFS approach:

- The MFS usually considers the boundary condition analytically or numerically defined. In the practical application of the present methodology, the known condition in the collocation points is the acceleration of vibration from a set of experimental measurements or, alternatively, the displacement of vibration obtained from the integration of acceleration records. This is the reason why the new method is called hybrid, since it combines vibration experimental measurements with a numerical approach. However, the method can also be used with numerically computed input boundary conditions if required.
- Typically, the MFS considers the same amount of virtual forces as collocation points. However, in order to enhance its computational performance, some MFS applications use an amount of virtual forces smaller than the amount of collocation points: although it is usual to consider a large amount of collocation points to accurately describe the boundary condition, the amount of virtual sources to accurately represent both the boundary condition and the response in the domain can be assumed quite smaller is some problems [37]. This implies that the system of equations becomes over-determined, requiring the use of a minimisation algorithm as a solver but

reducing the computational cost of the method. In the practical application of the present method, however, it is desirable that the amount of collocation points (sensors) should be always small. This implies that considering the same number of virtual forces as collocation points would not compromise significantly the computational efficiency. Thus, a minimisation algorithm would not be required.

- In contrast with the classical application of the MFS for exterior problems, in which the collocation points are enclosing the source, this methodology considers the collocation points to be located at the surface of the local sub-soil where the new structure will be constructed. Therefore, this method is based on enclosing the receiver instead of the source.

The proposed methodology consists of three steps. First step is explained with the support of Fig. 1, where Ω represents the soil domain and $d\Omega$ represents the ground surface where the particular building to be studied will be constructed, which corresponds also to the collocation points domain. The objective of this step is to determine the resulting vibration boundary condition at the collocation points due to the underground railway traffic. In this methodology, it is proposed to determine this boundary condition performing experimental measurements of the railway-induced vibrations using a setup of accelerometers (or other vibration sensors) as a set of collocation points distributed along $d\Omega$. The density and configuration of the distribution of these collocation points are studied in the present paper, since they strongly govern the accuracy of the boundary condition definition at $d\Omega$ and, as a consequence, the reliability of the proposed hybrid method. The time domain accelerations $\ddot{\mathbf{u}}_c$ at the collocation points given by the measurement setup can be transformed to frequency domain displacements $\mathbf{U}_c$ to get a discrete representation of the target boundary condition at $d\Omega$ in terms of displacement of vibration.

Important domains and surfaces for the second step of the methodology are illustrated in Fig. 2(a), where S is the surface that defines the domain of the virtual sources and Ω_s is the domain enclosed by S. Based on the indirect formulation of the boundary integral method, the boundary integral equation of this system for a single-layer potential representation can be written, in the frequency domain, as

$$U(\mathbf{r}) = \int_S H(\mathbf{r}, \mathbf{r}_s) T_v(\mathbf{r}_s) dS(\mathbf{r}_s), \tag{1}$$

where $U(\mathbf{r})$ represents the displacements of the soil at locations $\mathbf{r} = \{x\ y\ z\}^T$, which are restricted to the Ω_s domain, $T_v(\mathbf{r}_s)$ are the unknown tractions along the virtual boundary and $H(\mathbf{r}, \mathbf{r}_s)$ represents the Green's functions of the soil that relates the response at $\mathbf{r}$ due to a force applied along the S domain at $\mathbf{r}_s$, being $\mathbf{r}_s = \{x_s\ y_s\ z_s\}^T$ the location of the dS. Discretising the integral in Eq. (1) considering a set of virtual point sources to represent the unknown traction field in the boundary, these virtual forces can be computed as
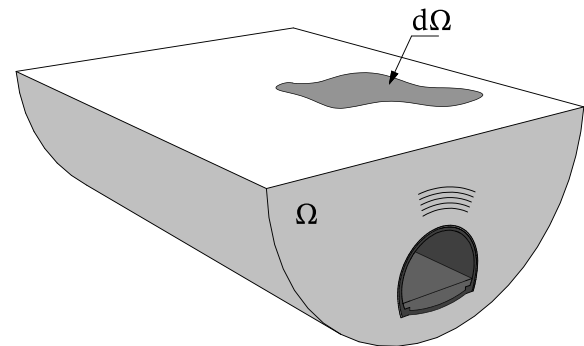

Fig. 1. Schematic representation of hybrid methodology first step: Evaluation of the boundary condition at the ground surface where the building will be constructed.
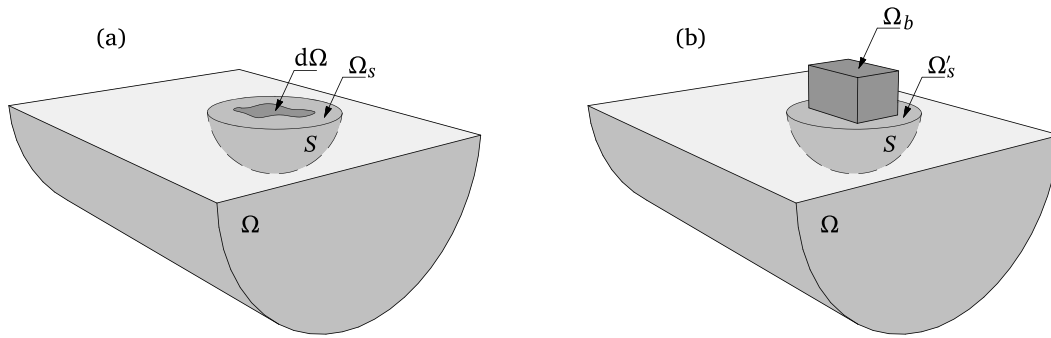
Fig. 2. Hybrid methodology schematic representation of steps 2 (a), equivalent source distribution, and 3 (b), building response.

$$\mathbf{F}_v = \mathbf{H}_{cf}^{-1}\mathbf{U}_c, \tag{2}$$

where $\mathbf{F}_v$ is a column vector that collects the virtual forces and $\mathbf{H}_{cf}$ is a receptance matrix that relates the virtual forces and the collocation points response obtained with a local subsoil model of the existing ground. The receptance matrix $\mathbf{H}_{cf}$ is square in the present method because of the consideration of the same number of sources as collocation points. Then, the response of the building-soil system can be obtained by

$$\mathbf{U}_b = \mathbf{H}_{bf}\mathbf{F}_v, \tag{3}$$

where $\mathbf{U}_b$ represents the response of a set of evaluation points placed in the building-soil model and $\mathbf{H}_{bf}$ is the receptance matrix that relates the virtual forces and the evaluation points response. The building-soil model is represented by joint building Ω_b and local sub-soil Ω_s' domains, as shown in Fig. 2(b), being Ω_s' the domain Ω_s after subtracting the building foundations. The $\mathbf{H}_{bf}$ matrix is obtained using the building-soil model specifically developed for the particular building to be studied. Suitable modelling approaches to be used in this regard are 3D FEM-PML models [24], 3D FEM-BEM approaches [15,38], semi-analytical modelling methods for 3D soil-building systems [39,40] or other hybrid options [23], among others.

The so-called *three-step solution* is a classical SSI method in which the problem is solved in three steps: the evaluation of the free field response of the soil at the soil-structure interface (kinematic interaction), the determination of the foundation equivalent stiffness and the computation of the dynamic response of the building supported by those equivalent stiffness and subjected to the base motion evaluated in the kinematic interaction step (dynamic interaction) [41]. In the context of this SSI problem solving architecture, the present approach provides various important benefits. First, the kinematic interaction is directly evaluated at the ground surface instead of at the soil-structure interface, making the procedure meshless, simple and standard for any foundation type. Furthermore, the incident wave field is here characterised by a set of virtual forces enclosing the structure which are computed in the second step of the proposed approach. Classical approaches transform the wave field into loads acting on the soil-structure interface, while in this method the virtual forces are located in the soil surrounding the structure, at S. The geometrical separation between the virtual forces and the soil-structure interface allows for controlling the effect of the structure foundations to these forces. Moreover, the virtual surface S where the forces are applied can be simply a semi-sphere (proposed in the present paper) rather than a geometrically complex soil-structure interface. Finally, the inclusion of the soil in the dynamic interaction step as a part of the model ensures an accurate representation of the foundation stiffness.

As previously mentioned, this method is based on a weak coupling between the railway infrastructure and the building. Therefore, it is assumed that the transfer functions between the locally surrounding soil and the building are not affected by the presence of the railway tunnel or

the at-grade track. Thus, this assumption will be invalid when the structure and the railway infrastructure are very close to each other. Coulier et al. [31] presented a study of the source-receiver coupling influence on the railway track compliance and on the dynamic transfer function between the source (a railway infrastructure) and the receiver (a building). In general, the study found that the source-receiver inter-action significantly affects the prediction of dynamic transfer functions between the source and the receiver for railway tunnels at a distance from a building smaller than the wavelength of the P-waves in the soil and for at-grade railway track closer than six wavelengths of the Rayleigh waves. However, it should be mentioned that these rules are related to the transfer functions between the track and the building, which are different from the transfer functions used in the present work.

3. Numerical validation of the methodology and parametric study for 2D problems

In this section, the previously explained hybrid method is numerically validated in a 2D point of view. Moreover, a parametric study is conducted in order to obtain a strategy for the selection of the amount of collocation points and the location of the virtual sources. In order to achieve this validation, various 2D FEM-PML models have been created, all of them based on the approach presented by Lopes et al. [7]. Thus, for this validation, Eqs. (2) and (3) are formulated in two dimensions. The study is presented in two sections: one related to case studies where the soil is assumed to be homogeneous (Sec. 3.1) and the other one where the case studies include a layered soil configuration (Sec. 3.2).

With the aim of performing this numerical study, $\mathbf{U}_c$ is obtained numerically by using a 2D model of a tunnel-soil system instead of using experimental measurements. The rest of the methodology follows the steps explained in Sec. 2, with the particularity of which the virtual sources are assumed to be uniformly distributed along a semi-circumference with centre located at the surface of the ground and in the middle of the building. This regular distribution is chosen since it allows for a general treatment of any type of building foundation and also follows general guidelines for the choice of virtual sources distribution presented by Alves et al. [42]. The number of collocation points and virtual sources is equal to N. Both horizontal and vertical degrees of freedom are considered. The radius of the semi-circumference of virtual sources is denoted by r. Moreover, a comprehensive 2D FEM-PML model of the tunnel-soil-building system, called the reference model, is used for each case study to check the numerical accuracy of the hybrid method. This accuracy is assessed by comparing the response obtained by this reference model at any evaluation point of the building or the surrounding ground with the response at the same points obtained by the hybrid methodology. In order to quantify the accuracy of the hybrid method, a global error parameter ε, associated with the response of the building in a particular point, is defined as

$$\varepsilon = \frac{1}{N_f} \sum_{i=1}^{N_f} \frac{U_{b_i}^r - U_{b_i}^h}{U_{b_i}^r}, \qquad (4)$$

where N_f is the number of frequency sampling points within the considered range of frequency, $U_{b_i}^r$ is the complex value of the displacement for the i-th frequency obtained by the reference model and $U_{b_i}^h$ is the complex value of the displacement for the i-th frequency computed with the hybrid method. In this work, the considered frequency range is from 1 Hz to 80 Hz, as it is the standard frequency range for ground-borne vibration in buildings [43].

3.1. Case studies with homogeneous soil profiles

The overall system geometry considered for the case studies with homogeneous soil profiles is presented in Fig. 3. This system consists of a two-storey building with shallow foundations placed near an underground railway infrastructure and where the soil is considered to be a homogeneous elastic half-space.

The building is here assumed to be infinite in the longitudinal direction, as well as for the rest of case studies considered in this work. This assumption is taken to reduce the computational requirements of a fully 3D tunnel-soil-building dynamic problem, allowing for the development of parametric studies. The mechanical properties of the different sub-systems are defined in Table 1, where three different soil stiffness are shown, defining the three case studies that are going to be studied in this section. In that table, ρ, E, ν and η represent the density, the Young's modulus, the Poisson's ratio and the structural damping of the material of the corresponding sub-system, respectively.

The railway underground infrastructure considered consists of a tunnel with 8.5 m of inner diameter and a lining thickness of 0.35 m. Thus, on the one hand, the reference models used in this section are based on 2D FEM-PML meshes of the comprehensive geometry presented in Fig. 3. On the other hand, the models used for the hybrid method are based on 2D FEM-PML meshes of the required parts of the overall system shown in Fig. 4, always keeping the configuration of the original geometry.

Therefore, a total of four FEM-PML meshes based on 8-noded quadrilateral finite elements (FE) are constructed for each case:

- The mesh for the reference model, which consists of the tunnel, the homogeneous soil and the building. The system to be meshed is
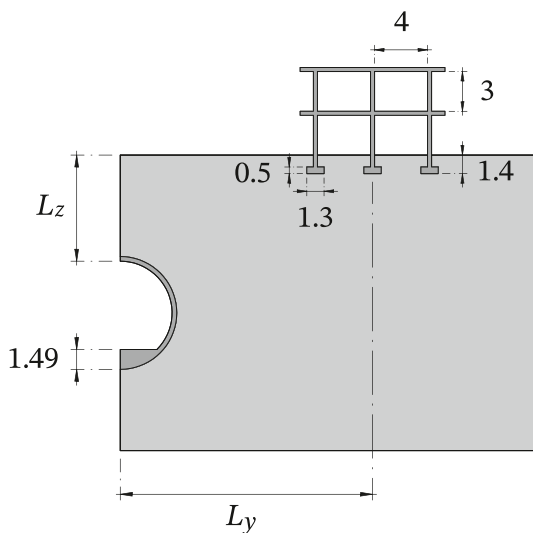

Fig. 3. Geometry of the tunnel-soil-building system assumed for the homogeneous half-space case studies, referred to as the reference model. Distances in meters.

Table 1
Mechanical properties used for the different sub-systems for the cases with homogeneous soil.

Sub-system	ρ [kg/m^3]	E [MPa]	ν [−]	η [−]
Soil A	2000	195	0.3	0.04
Soil B	2000	290	0.3	0.04
Soil C	2000	350	0.3	0.04
Tunnel	2500	30,000	0.2	0.01
Building	2500	30,000	0.2	0.01

presented in Fig. 3. The system is considered to be symmetric with respect to the tunnel centre. This property is exploited to reduce the computational effort by meshing only half of the system. For this case, the PML boundaries are located at 12.5 m horizontally away from the building centre and at 7.6 m vertically away from the tunnel invert. The FE used for the soil, the tunnel and the building have an edge length of 0.3 m, 0.35 m and 0.4 m, approximately. These FE sizes apply for all the meshes created in this work. Regarding the size of the FE in the soil, it is computed ensuring at least six FE per wavelength for all the soil cases until 200 Hz. Due to the symmetry, the model is considering two mirror buildings. However, as the dynamic coupling between the two symmetric buildings is found to be insignificant as compared with the tunnel-building coupling, that mirror building structure becomes irrelevant.

- The mesh of the tunnel-soil system, which is used to obtain numerically $\mathbf{U}_c$. The domain to be meshed is presented in Fig. 4(a). The symmetry of the problem is also exploited for this mesh. The geometrical definition of the mesh is the same as the reference model mesh, except for the absence of the building.

- The mesh of the soil system in the absence of the tunnel and the building, which is used to obtain $\mathbf{H}_{cf}$. The system to be meshed is presented in Fig. 4(b). For this case, the PML boundaries are located at 12.5 m horizontally away from the centre of the mesh (in this case, at both sides) and also at 12.5 m vertically away from the ground surface.

- The mesh of the building-soil system (Fig. 4(c)), which is used to compute $\mathbf{H}_{bf}$. The geometrical definition of this mesh is the same as the previous one, except for the inclusion of the building mesh with the exact same configuration as the one appearing in the reference model.

For all the case studies, the excitation assumed consists of a vertical unitary force applied on the tunnel invert and at 69 cm horizontally away from the centre of the tunnel. Moreover, the same evaluation point is used along this work, which is the mid-span point of the building first floor on the right side. Due to unitary force consideration, the displacement results at the evaluation point are the receptance frequency response functions associated with those degrees of freedom.

In Figs. 5 and 6, a comparison between the reference model results and the hybrid model results is shown for Soil A and Soil C case studies, respectively, for vertical and horizontal response at the evaluation point, for the closest and farthest tunnel-soil separation cases and for three hybrid method configurations: Case 1, with $N = 12$ and $r = 6$ m, which implies a distance between virtual sources of 1.7 m; Case 2, with $N = 32$, $r = 12$ m and a distance between virtual sources of 1.2 m; and Case 3, with $N = 32$, $r = 6$ m and a distance between virtual sources of 0.6 m.

For the cases considered, the hybrid method results match quite accurately with the reference model results until 80 Hz. Above this frequency, there are significant differences between both methods depending on the case. For Soil A case study, Case 3 is giving accurate hybrid method results for the whole frequency range. In contrast, the results for Cases 1 and 2 start to be incorrect for frequencies greater that 100 Hz and 160 Hz, respectively. Those frequencies are related to S-wave wavelengths of 1.94 m and 1.21 m, respectively. Comparing these values with the distances between virtual sources previously mentioned,
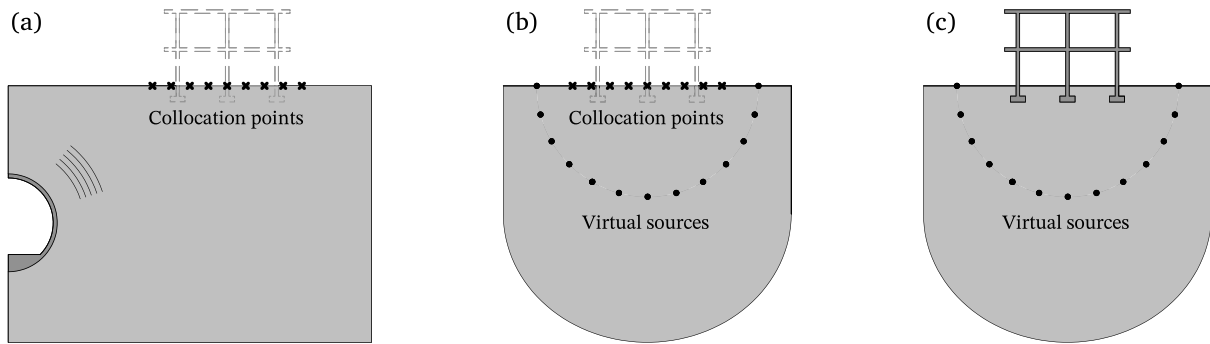
Fig. 4. Tunnel-soil (a), only soil (b) and building-soil (c) models considered for the hybrid method application in the context of the case studies with homogeneous soil profiles. Cross and circular point markers are representing the collocation points and the virtual sources, respectively.
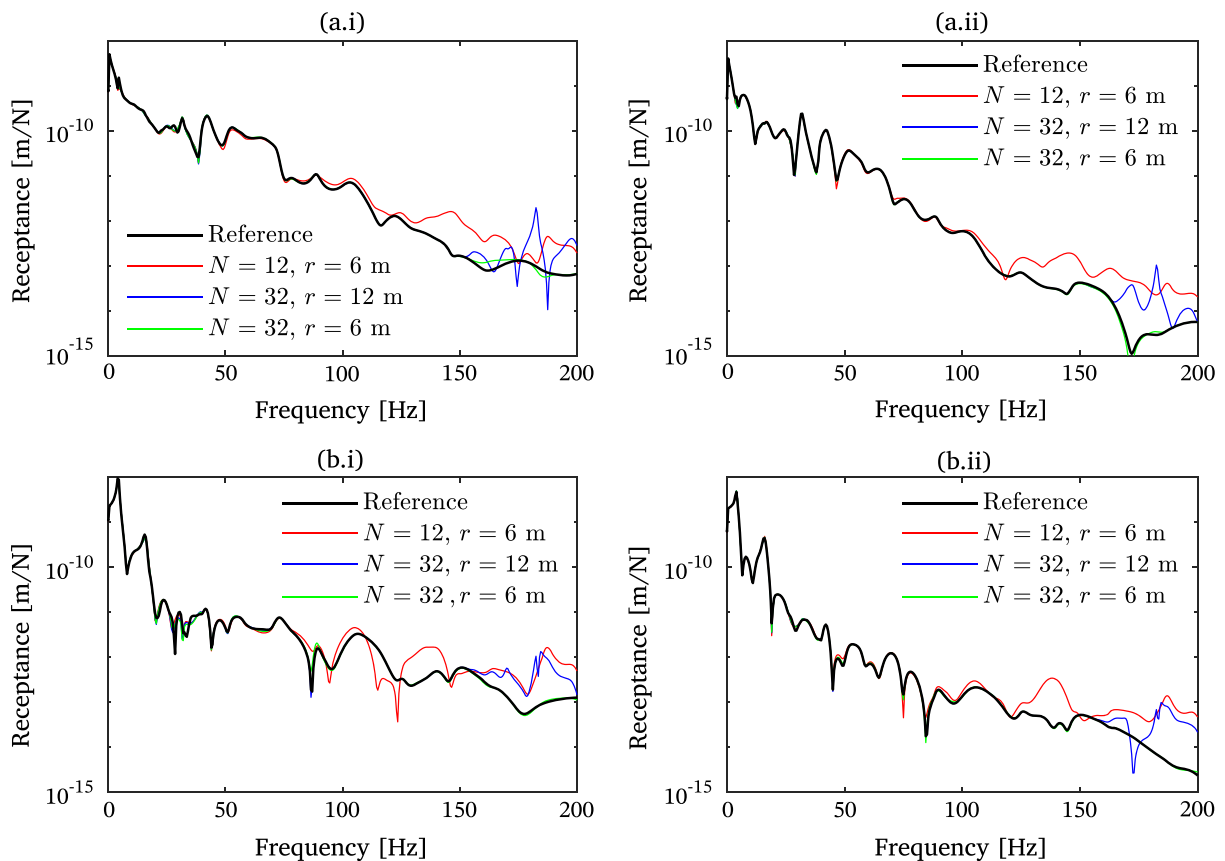

Fig. 5. Amplitude of the receptance for the vertical (a) and horizontal (b) response at the evaluation point. The black curve corresponds to the reference model results. The red, blue and green curves are obtained with the hybrid method for the Case 1, Case 2 and Case 3, respectively. Figures (i) are associated with the case where $L_z = 8$ m and $L_y = 19$ m and figures (ii) are associated with $L_z = 20$ m and $L_y = 30$ m. These results are associated with the Soil A case study. For interpretation of the references to colour in this figure legend, the reader is referred to the Web version of this article.

a general relation for the correctness of the hybrid method in 2D problems can be established: the distance between virtual sources d should be smaller than the S-wave wavelength corresponding to the higher frequency of the desired frequency range, referred in this work as λ_s. For the Soil C case study, Cases 2 and 3 show a good agreement with the reference model until 200 Hz. Only the Case 1 has discrepancies with the reference model results above 140 Hz, which is associated with a S-wave wavelength of 1.85 m. As also observed in the results of the Soil A case study, the empirical rule for the correctness of the hybrid method tends to be $d < \lambda_s$.

In order to verify this empirical rule and also to study the influence of r on the method accuracy, a parametric study has been conducted.

Previous studies have pointed out that MFS faces numerical instabilities for short distances between virtual sources and collocation points that result in loss of accuracy of the method, while large distances lead to large ill-conditioning issues and even its failure [42]. Thus, a study of the influence of r on the results of the present method should provide insights of adequate values of this distance to significantly avoid both these two undesirable numerical problems. In the framework of this parametric study, the top of the tunnel is assumed to be located at a variable distance L_z from the ground surface, which takes the values of 8 m, 10 m, 15 m and 20 m. The horizontal distance from the centre of the building to the centre of the tunnel L_y is also variable and takes the values of 19 m, 22.5 m, 25 m and 30 m. For each combination of
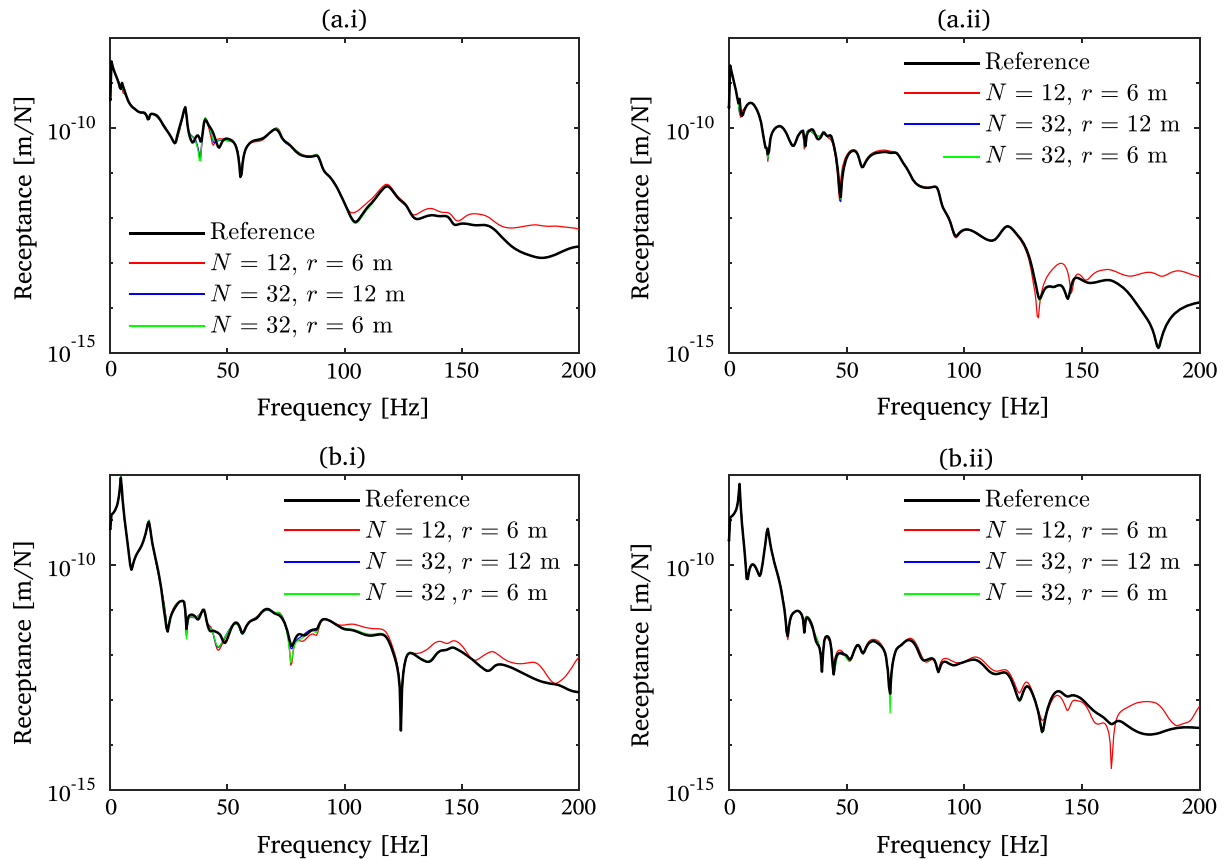
Fig. 6. Amplitude of the receptance for the vertical (a) and horizontal (b) response at the evaluation point. The black curve corresponds to the reference model results. The red, blue and green curves are obtained with the hybrid method for the cases of Case 1, Case 2 and Case 3, respectively. Figures (i) are associated with the case where $L_z = 8$ m and $L_y = 19$ m and figures (ii) are associated with $L_z = 20$ m and $L_y = 30$ m. These results are associated with the Soil C case study. For interpretation of the references to colour in this figure legend, the reader is referred to the Web version of this article.

distances L_z and L_y, a particular parametric study considering N and r as variables is performed for the three case studies introduced. Specifically, N and r are taking integer values ranging from 4 to 33 and from 6 to 12, respectively. The range of values for r has been imposed by the geometrical restrictions given by the building foundations, resulting on lower r limit of 6 m, and the tunnel location, giving an upper r limit of 12 m. The results for this parametric study in terms of the global error ϵ, computed using Eq. (4), are shown in Fig. 7, Fig. 8 and Fig. 9, for the Soil A, Soil B and Soil C case studies, respectively. For the global error, only the vertical component of the displacement at the evaluation point is taken into account, since results associated with the horizontal component have been found to follow the same trend.

Three important conclusions can be observed from the results of this parametric study. Firstly, as a general trend, minimal errors of the method decrease as the soil stiffness and the distance between the tunnel and the building increase. As explained before, this happens because the interaction between the tunnel and the building gains relevancy as the ratio between the building-tunnel distance and the wavelength λ_s becomes smaller. It is also interesting to observe that the horizontal component of the building-tunnel distance has a stronger impact on the building-tunnel dynamic interaction, probably because of the relevancy of the Rayleigh waves on the elastic wave propagation from the tunnel to the building. Secondly, large errors of the method are found below the straight line defined by distances between virtual sources equal to λ_s, which is in direct correspondence with the empirical rule previously stated. Thus, that empirical rule is validated for the case studies presented in this section. Finally, for values of r resulting in virtual sources particularly close to the building foundation (at less than 1 m), the method loses accuracy, since the influence of the building foundation to

the virtual forces increases its significance.

3.2. Case studies with layered soil profiles

In this section, two new case studies based on layered soil profiles are introduced. These new cases are called Layered A and Layered B and their layouts are shown in Fig. 10(a) and Fig. 10(b), respectively. The parametric study configuration presented in the previous section has been also applied to these two case studies. For the Layered B case, only a vertical distance L_z of 8 m is considered in the parametric study due the geometrical restrictions imposed by the layer. The 2D FEM-PML meshes constructed to perform the parametric study are identical to the ones presented for the homogeneous soil case studies in Sec. 3.1 with the exception of the layer inclusion. The material properties associated with these two new case studies are shown in Table 2.

The results of the parametric study for Layered A and Layered B cases are shown in Figs. 11 and 12, respectively. In these plots, the limits of the empirical rule $d < \lambda_s$ considering the parameters of the upper layer and the lower layer are illustrated by dashed and dashed-dotted lines, respectively. As expected, taking the wavelength λ_s associated with the upper layer for the empirical rule ensures the correct performance of the hybrid methodology, while the use of the lower layer λ_s could result in highly inaccurate predictions. It can also be seen that the thicker (with respect to the tunnel-building distance) the upper layer is, the higher its influence on the method performance becomes. In contrast, when the tunnel-building vertical distance is significantly larger than the layer thickness, the influence of this layer is small. Thus, the empirical rule considering the parameters of the upper layer is too restrictive only for cases where L_z is large, as can be especially seen in plots (d) of Fig. 11. It
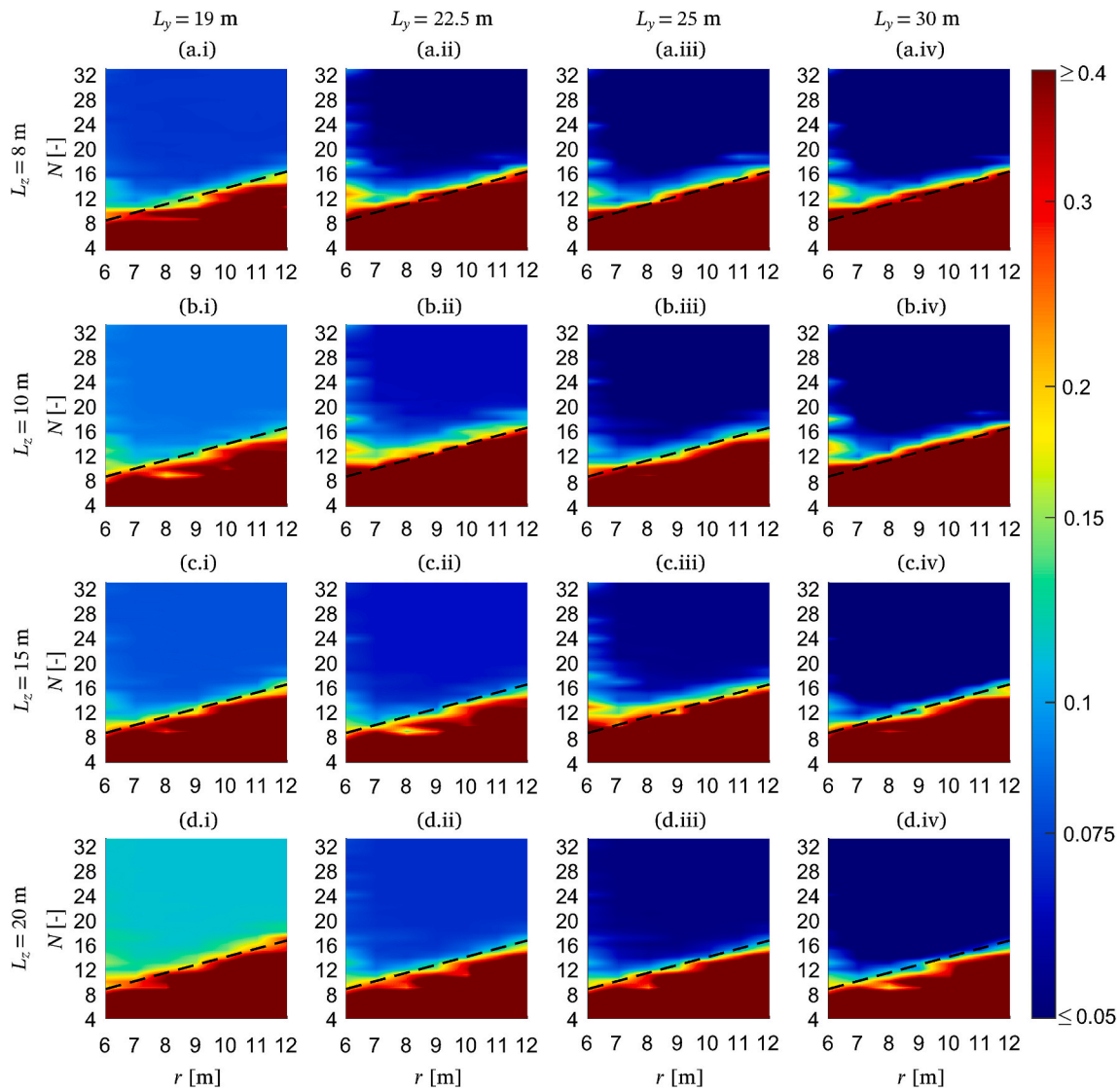
Fig. 7. Global error ε for the parametric study performed in the context of Soil A case study. Plots denoted by (a), (b), (c) and (d) are related to L_z equal to 8 m, 10 m, 15 m and 20 m, respectively. Plots denoted by (i), (ii), (iii) and (iv) are related to L_y equal to 19 m, 22.5 m, 25 m and 30 m, respectively. Black dashed lines represent a distance d equal to λ_s.

should be noted that, in this layered soil scenarios, virtual sources are often located at different layers. However, the method handles this naturally, performing with similar accuracy to homogeneous half-space cases.

4. Numerical validation of the methodology and parametric study for 2.5D problems

In this section, the previously explained hybrid method is validated numerically in a 2.5D point of view. This verification is based on the comparison of the results of the hybrid method with the responses provided by a fully numerical reference model in several 2.5D case studies, following the same idea of the verification studies for 2D problems described in the previous section. A parametric study for the 2.5D case studies considered is also conducted in this section. The aim of this study is to test the correctness of the empirical rule previously developed in the context of 2D problems as a strategy for the selection of N and r in general 3D scenarios. The 2D FEM-PML models used for the simulations presented in the previous section are also used here for 2.5D studies by simply considering wavenumbers different than zero. Thus, in this framework, Eqs. (2) and (3) are assumed to be formulated in the

wavenumber-frequency domain.

4.1. Case studies with homogeneous soil profiles

For the numerical study presented in this section, the model and the meshes described in Sec. 3.1 for Soil A and Soil C cases are used. Two types of output results are examined in the framework of this numerical validation. On the one hand, the 2.5D Green's functions of the system associated with the same force and evaluation point considered in the 2D examples are obtained for frequencies ranging between 0 Hz and 80 Hz and for wavenumbers between 0 and 100 rad/m. On the other hand, the receptance at an arbitrary longitudinal coordinate x_0 due to a point load located at the same longitudinal point is computed by Fourier anti-transforming the 2.5D Green's functions using the expression

$$H(\omega) = \frac{1}{\pi} \int_0^\infty \overline{H}(k_x, \omega) \, dk_x, \tag{5}$$

where $\overline{H}(k_x, \omega)$ represents the 2.5D Green's function and $H(\omega)$ the computed receptance. For a vertical load, as it is considered in this work, this expression is only valid for y and z components of the response, while the x component is zero due to the symmetry conditions of the
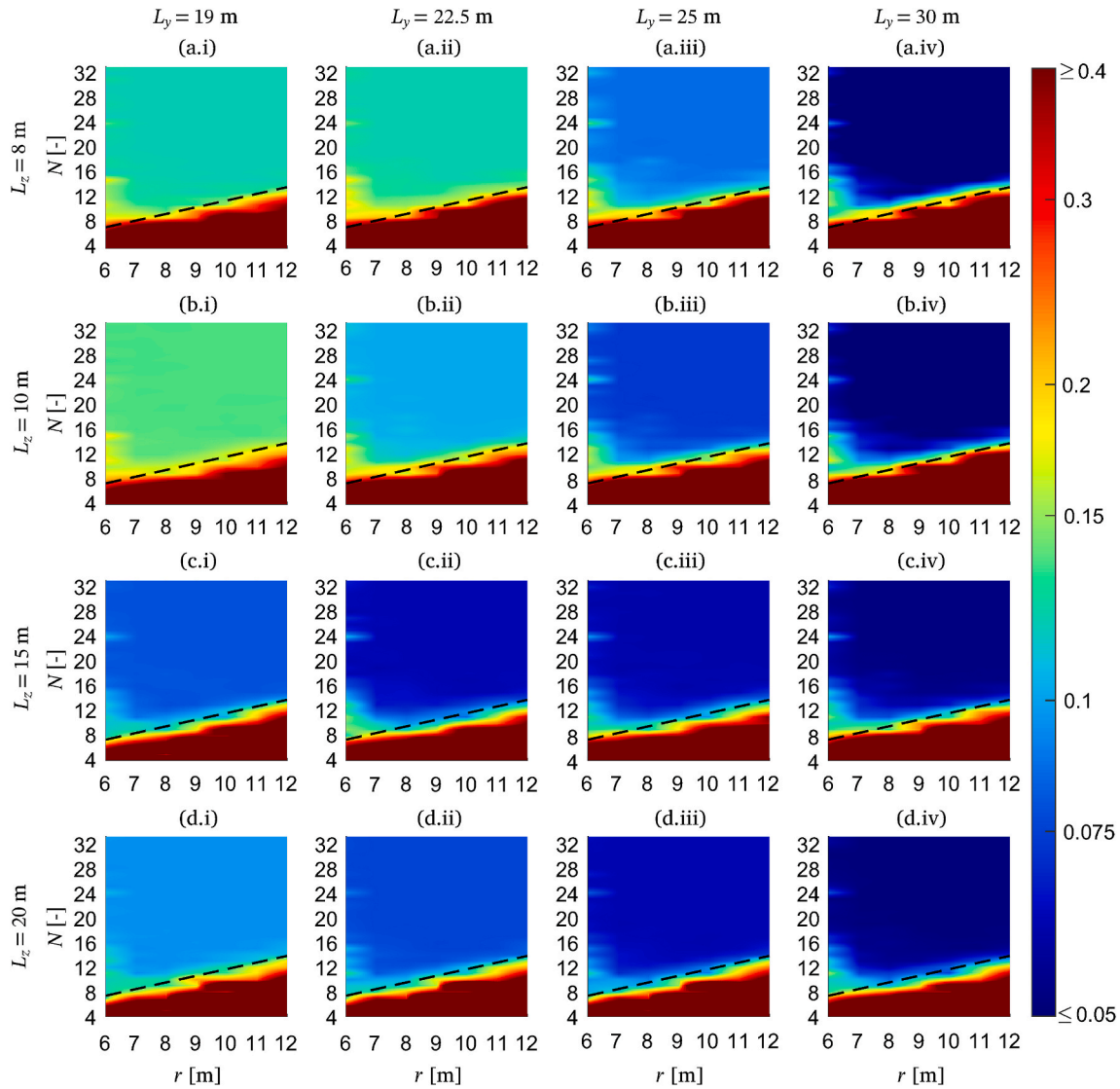
Fig. 8. Global error ε for the parametric study performed in the context of Soil B case study. Plots denoted by (a), (b), (c) and (d) are related to L_z equal to 8 m, 10 m, 15 m and 20 m, respectively. Plots denoted by (i), (ii), (iii) and (iv) are related to L_y equal to 19 m, 22.5 m, 25 m and 30 m, respectively. Black dashed lines represent a distance d equal to λ_s.

problem. The previous integration is numerically estimated using a trapezoidal rule over 1025 logarithmically spaced samples. As receptance values are computed using the whole information whitin the wavenumber spectrum, it can be used to verify the 3D correctness of the proposed method. However, highly accurate receptance results do not directly imply high accuracy of the 2.5D Green's functions across the wavenumber spectrum, since some localised errors along that spectrum can be covered up depending on the longitudinal load distribution considered. Thus, in order to fully assess the goodness of the proposed hybrid method, both receptance and 2.5D Green's function results are accounted for in this verification.

Fig. 13 presents a comparison between the receptance obtained with the reference model and the hybrid model for various configurations of virtual sources and in two main scenarios: the case study that considers Soil A profile and the largest tunnel-soil distance ($L_z = 20$ m and $L_y = 30$ m), representing the situation of lowest tunnel-building dynamic coupling, and the case study where Soil C profile is adopted together with the lowest tunnel-soil distance ($L_z = 8$ m and $L_y = 19$ m), representing the situation where the strongest tunnel-building dynamic coupling is expected. The comparisons are done for vertical and horizontal responses at the evaluation point and for three configurations of

virtual forces: Case 4, with $N = 7$ and $r = 7$ m, which implies a distance between virtual sources of 3.7 m; Case 5, with $N = 15$, $r = 12$ m and a distance between virtual sources of 2.7 m; and Case 6, with $N = 21$, $r = 7$ m and a distance between virtual sources of 1.1 m.

For the case with the weakest tunnel-building coupling, results associated with Case 6 are matching accurately with the results of the reference model for all the frequency range of interest, as predicted by the empirical rule $d < \lambda_s$, since $\lambda_s = 2.42$ m. In accordance, Case 5 results are incorrect for frequencies above 70 Hz, since λ_s at this frequency is approximately 2.77 m. Case 4 results show loss of agreement for frequencies above 45 Hz, while the empirical rule is predicting an accurate performance of the method until 52 Hz. For the case of the strongest tunnel-building coupling, only the Case 4 should bring inaccurate results according to the rule. However, due to the tunnel-building dynamic coupling, slight discrepancies between the hybrid method and the reference model results are arising along the frequency range, specially at 2 Hz and around 40 Hz for the vertical component, reaching maximum discrepancies of ±1.5 dB.

The verification results in the wavenumber-frequency domain for the case studies adopted in this section are shown in Fig. 14, for the case of the weakest tunnel-building dynamic coupling, and in Fig. 15, for the
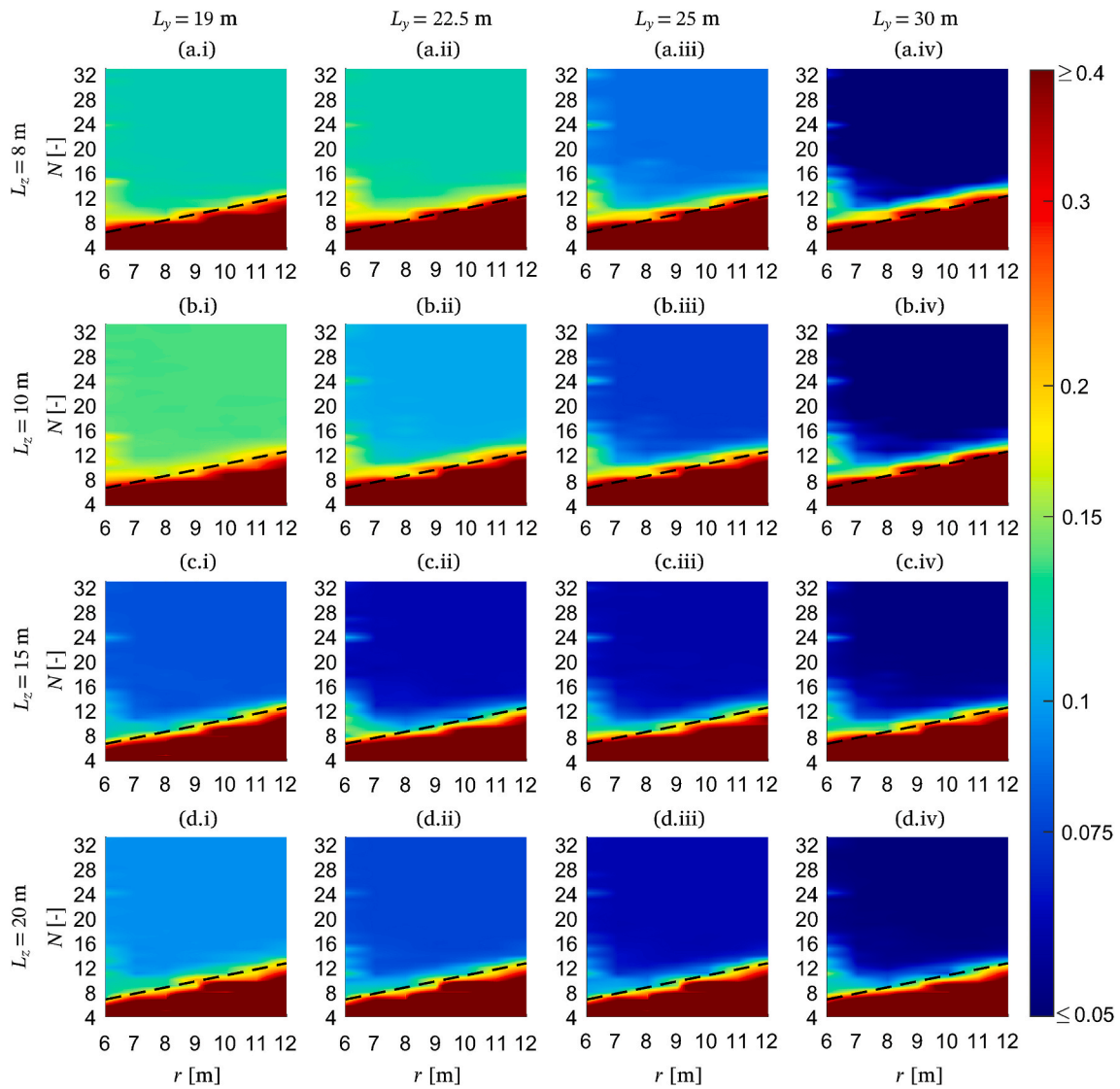
Fig. 9. Global error ε for the parametric study performed in the context of Soil C case study. Plots denoted by (a), (b), (c) and (d) are related to L_z equal to 8 m, 10 m, 15 m and 20 m, respectively. Plots denoted by (i), (ii), (iii) and (iv) are related to L_y equal to 19 m, 22.5 m, 25 m and 30 m, respectively. Black dashed lines represent a distance d equal to λ_s.
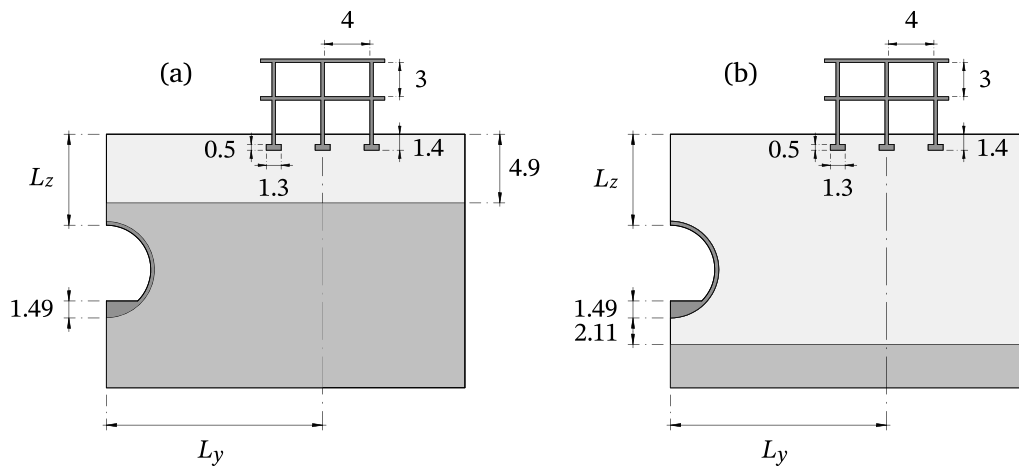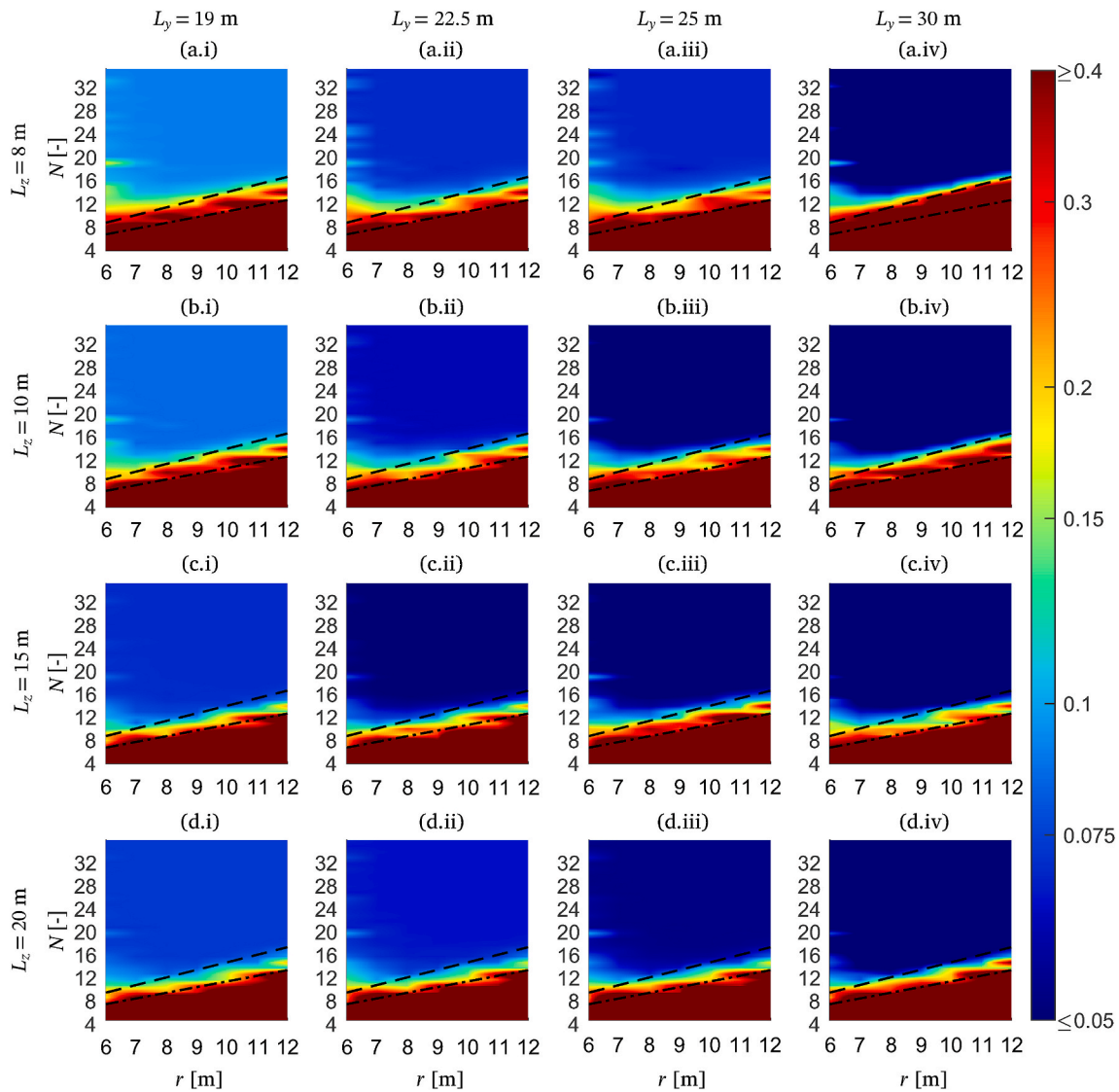

Fig. 10. Geometry of the tunnel-soil-building system assumed for the layered half-space case studies, which is based on 2-layer half-space where the layer interface is located above (a) or below (b) the tunnel. Distances in meters.

Fig. 11. Global error ε for the parametric study performed in the context of Layered A case study. Plots denoted by (a), (b), (c) and (d) are related to L_z equal to 8 m, 10 m, 15 m and 20 m, respectively. Plots denoted by (i), (ii), (iii) and (iv) are related to L_y equal to 19 m, 22.5 m, 25 m and 30 m, respectively. Black dashed and black dashed-dotted lines represent a distance d equal to λ_s associated with the upper and lower layers, respectively.

Table 2
Properties used for the different materials for the cases with a layered soil.

Sub-system	ρ [kg/m³]	E [MPa]	ν [−]	η [−]
Upper layer	2000	195	0.3	0.04
Lower half-space	2000	350	0.3	0.04
Tunnel	2500	30,000	0.2	0.01
Building	2500	30,000	0.2	0.01

case of the strongest coupling. These figures are illustrating the relative error between the reference model and the hybrid method associated with the 2.5D Green's functions. This error is computed using Eq. (4) for each discrete value of the 2.5D Green's functions along the frequency and wavenumber samplings, avoiding the average along frequency. For the wavenumber, only the range between 0 and 2 rad/m is considered, since it is where the spectral content is mostly concentrated. Two values for r (7 m and 12 m) and four for N (7, 12, 15 and 21) are considered in the study.

Results are pointing out that large r values imply high correctness of the hybrid method at high wavenumbers. This can be seen comparing plots (a.ii) and (b.iv), which are associated with similar distances

between sources ($d \approx 2$ m). The errors associated with the tunnel-building dynamic coupling can be clearly observed in Fig. 15 in the form of an error distribution pattern at wavenumbers smaller than one. These errors at low wavenumbers are always there, regardless of the amount of virtual sources. Comparing these results with the ones obtained in Fig. 13(a.ii), two issues arise: the errors at high wavenumbers are not significantly affecting the receptance results in these cases due to the high decay of the 2.5D Green's functions along wavenumber; and the large but localised errors due to the tunnel-building coupling shown in the 2.5D Green's functions lead to small discrepancies in the receptances due to the average introduced by the Fourier transform from the wavenumber to the space domain.

4.2. Case studies with layered soil profiles

Finally, the verification study procedure presented in the previous section has been also applied for the case of the Layered A case study and two tunnel-building relative positions: $L_z = 8$ m and $L_y = 19$ m; $L_z = 8$ m and $L_y = 30$ m. Verification results associated with the receptance frequency response function are shown in Fig. 16.

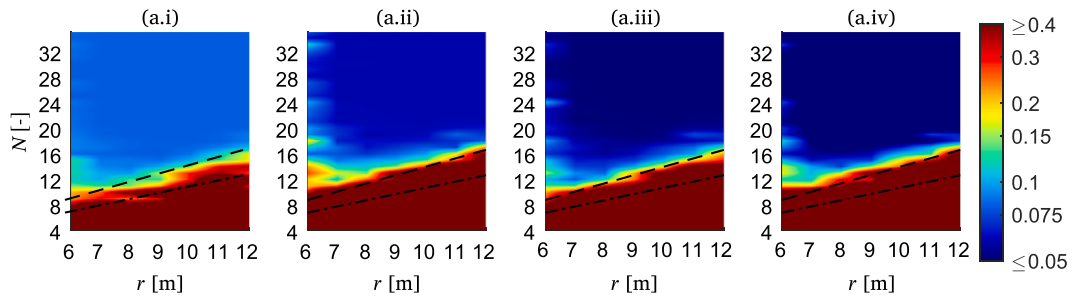In terms of virtual source distribution, results show a similar trend as

Fig. 12. Global error ε for the parametric study performed in the context of Layered B case study. Plots denoted by (i), (ii), (iii) and (iv) are related to L_y equal to 19 m, 22.5 m, 25 m and 30 m, respectively. Black dashed and black dashed-dotted lines represent a distance d equal to λ_s associated with the upper and lower layers, respectively.
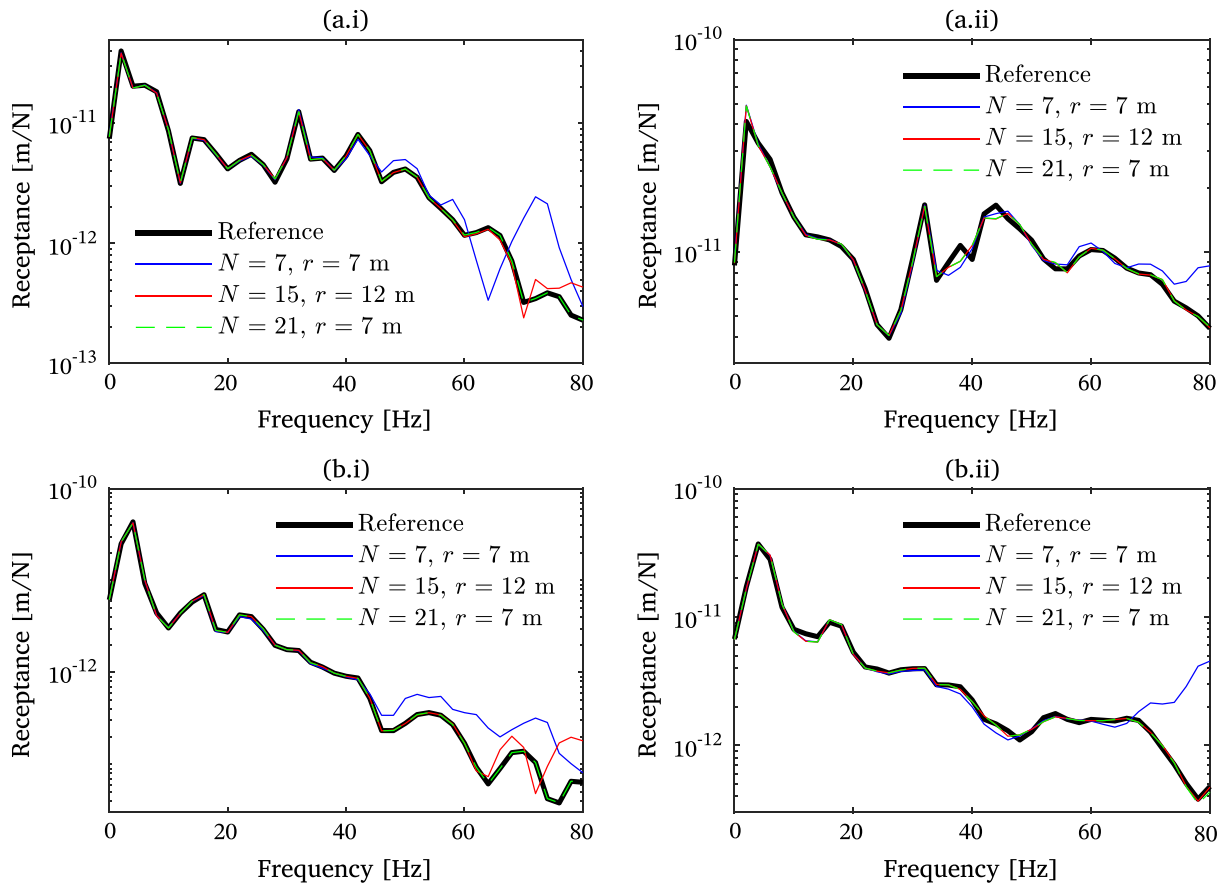

Fig. 13. Amplitude of the receptance for the vertical (a) and horizontal (b) response at the evaluation point. The black curve corresponds to the reference model results. The blue, red and green lines represent the results of the hybrid method for the Case 4, Case 5 and Case 6, respectively. Figures (i) are associated with the case where $L_z = 20$ m, $L_y = 30$ m and Soil A and figures (ii) are associated with $L_z = 8$ m, $L_y = 19$ m and Soil C. For interpretation of the references to colour in this figure legend, the reader is referred to the Web version of this article.

the results observed in the homogeneous Soil A case, since the frequency ranges of correctness for the Case 4 and Case 5 configurations are very similar to the ones observed in Fig. 13(a.i) and Fig. 13(b.i). These observations are in accordance with the findings provided by the parametric study conducted for the 2D Layered A case study (Fig. 11), where it can be seen that, for $L_z = 8$ m, the empirical rule based on the upper layer mechanical properties allows for an appropriate design of r and N. Regarding the influence of the tunnel-building coupling, the case with $L_y = 30$ m is strongly insensitive to that phenomenon while the case of $L_y = 19$ m shows a significant discrepancy at 2 Hz (commonly a frequency of poor interest in railway-induced vibration problems) of 3.4 dB and slight discrepancies smaller than 1 dB from 26 Hz to 36 Hz. In general, it can be stated that hybrid method is providing highly accurate results for

the Case 6 configuration.

The results regarding the verification based on the 2.5D Green's functions are shown in Fig. 17 for the case of $L_y = 19$ m and in Fig. 18 the case of $L_y = 30$ m. As shown in the previous section for the homogeneous soil cases, a larger radius ensures smaller errors of the hybrid method, as it can be seen from the comparisons of plot (a.i) against (b.ii) and (a.ii) against (b.iv). Moreover, the errors associated with the tunnel-building dynamic coupling are observed in most of the figures (except in the ones with high error density) of the same case study with a persistent error distribution pattern appearing at low wavenumbers. Thus, this pattern is clearly less intense in the case of $L_y = 30$ m than in the case of $L_y = 19$ m, since the dynamic coupling is correspondingly less significant in the former than in the latter. It can be also observed large errors at high
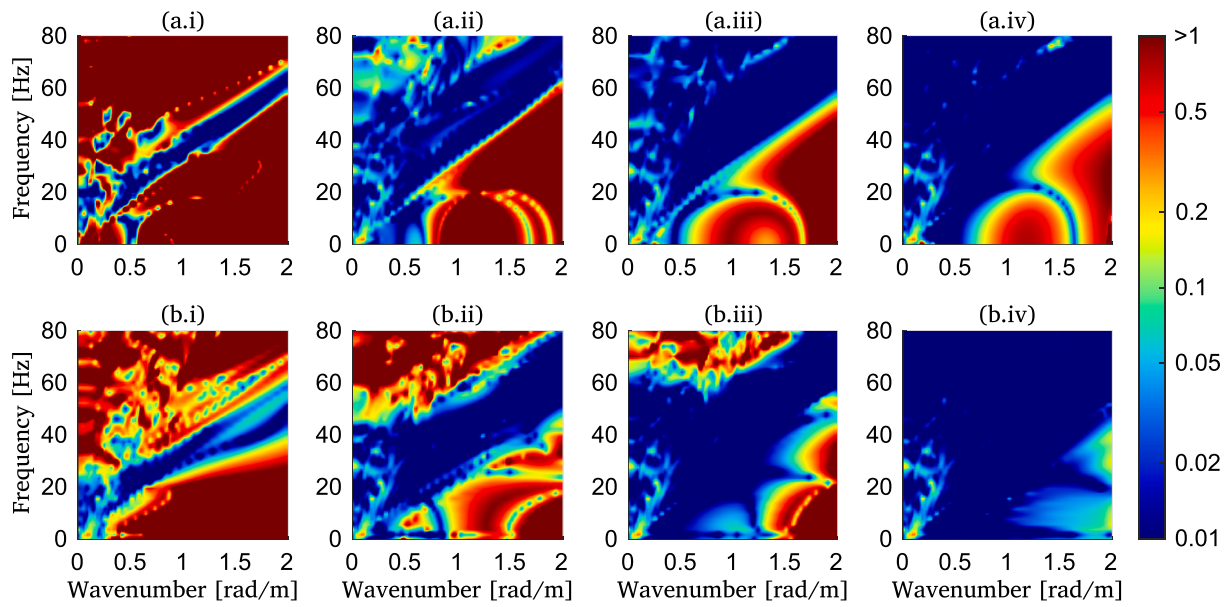
Fig. 14. Relative error of hybrid methodology for the Soil A, L_z equal to 20 m and L_y equal to 30 m. Plots denoted by (a) and (b) are related to r equal to 7 m and 12 m, respectively. Plots denoted by (i), (ii), (iii) and (iv) are related to N equal to 7, 12, 15 and 21, respectively.
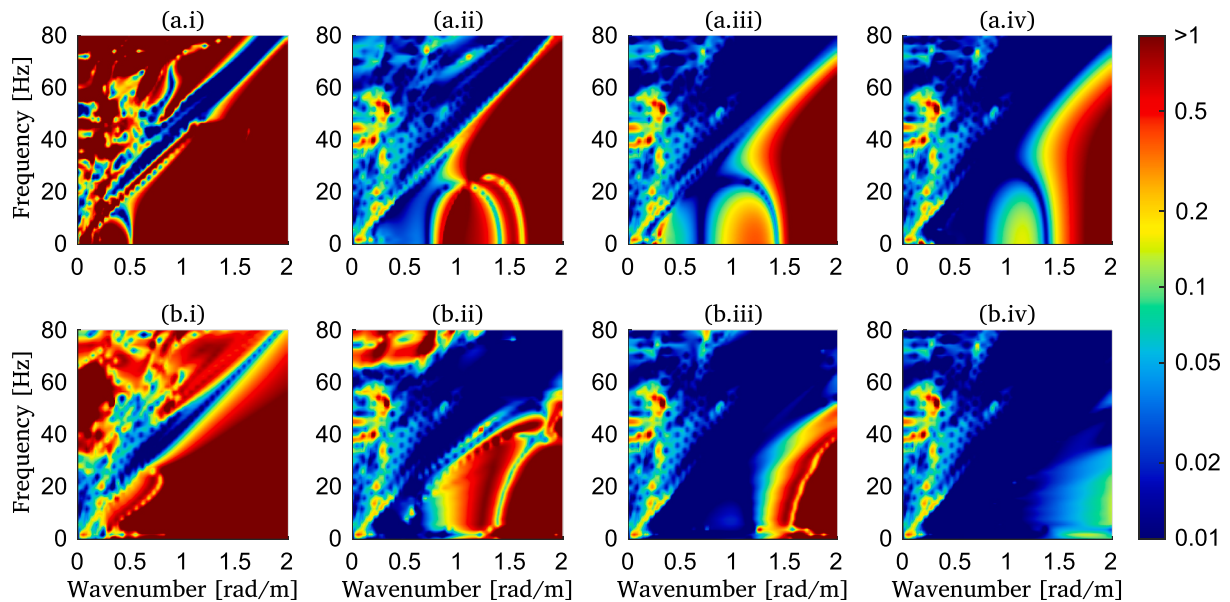

Fig. 15. Relative error of hybrid methodology for the Soil C, L_z equal to 8 m and L_y equal to 19 m. Plots denoted by (a) and (b) are related to r equal to 7 m and 12 m, respectively. Plots denoted by (i), (ii), (iii) and (iv) are related to N equal to 7, 12, 15 and 21, respectively.

wavenumbers for the case of $L_y = 30$ m. These errors are of numerical nature, due to the large decay of the 2.5D Green's functions along the wavenumber for this specific case, and this is the reason they are not affecting at all the accuracy of the receptance estimation. This decay is more pronounced in this case because the waveguide that the upper layer represents highly concentrates the wavenumber spectral content at low wavenumbers.

5. Conclusions

In this paper, a new methodology for the prediction of railway-induced vibration in buildings to be build close to an operational railway infrastructure is proposed. This is a hybrid approach, since: it uses experimental measurements of the railway-induced vibration in the

ground surface to obtain the incident wave field; and it employs a theoretical building-soil model to obtain the vibration response of the building structure due to railway traffic. The method is based on the assumption of a weak coupling between the railway infrastructure and the building structure. In this paper, the proposed methodology is numerically validated in a set of 2D and 2.5D case studies. To ensure that the methodology application is providing accurate results, it is found that the distance between virtual sources should be smaller than the S-wave wavelength of the upper soil layer corresponding to the highest frequency of the frequency range of interest. Results obtained in all case studies presented that complies with this empirical rule are showing a strong agreement between the new proposed hybrid method and a full numerical model of the system which has been used as a reference. For soil profiles where the upper layer is small with respect to the tunnel-
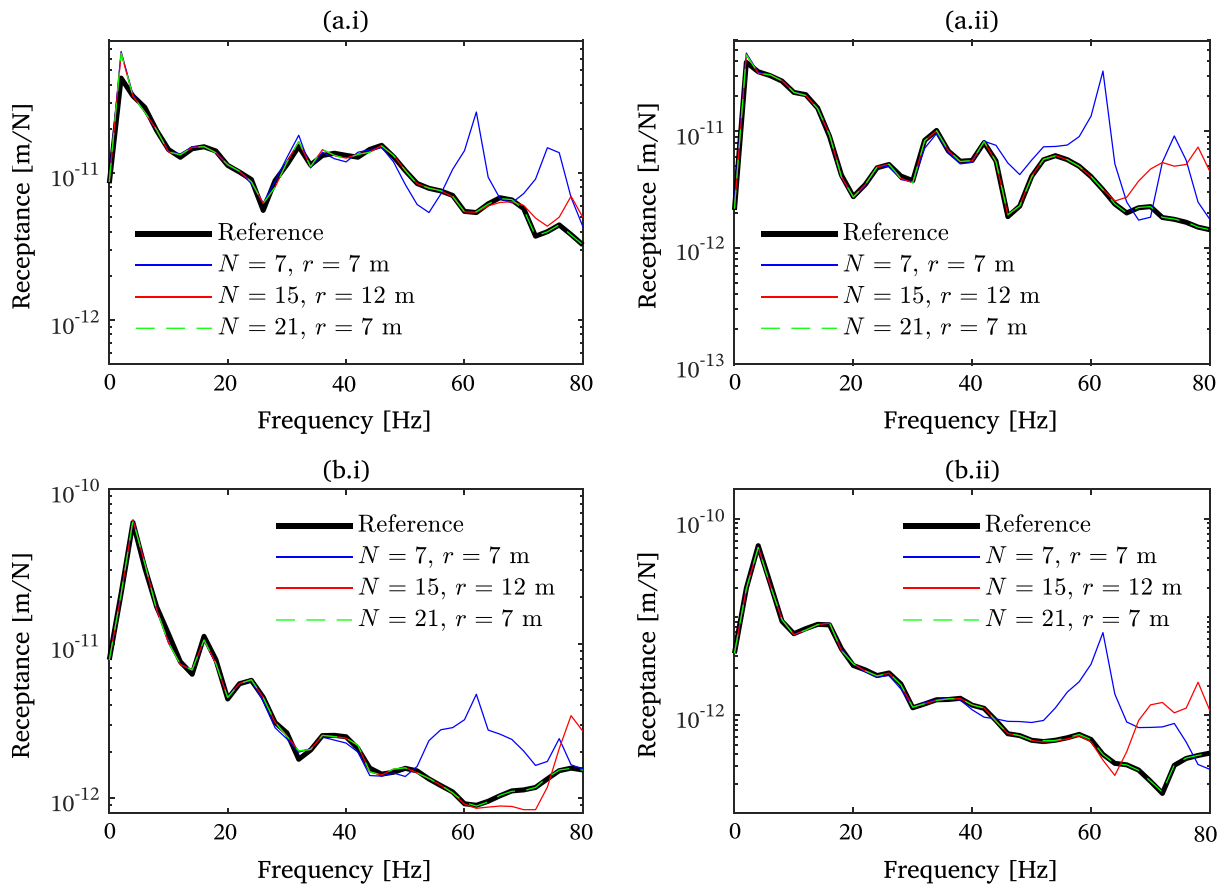
Fig. 16. Amplitude of the receptance for the vertical (a) and horizontal (b) response at the evaluation point. The black curve corresponds to the reference model results for the Layered A case study. The blue, red and green lines represent the results of the hybrid method for the Case 4, Case 5 and Case 6, respectively. Figures (i) are associated with the case where $L_z = 8$ m and $L_y = 19$ m and figures (ii) are associated with $L_z = 8$ m and $L_y = 30$ m. For interpretation of the references to colour in this figure legend, the reader is referred to the Web version of this article.
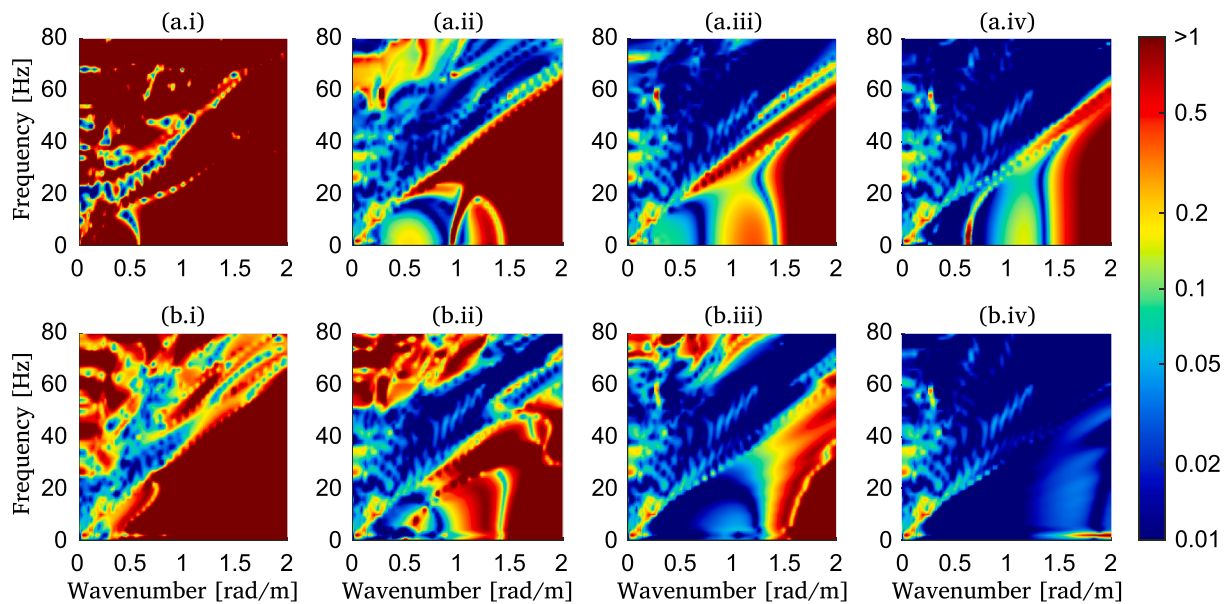
Fig. 17. Error ε for the parametric study performed in the context of Layered A case study and for L_z equal to 8 m and L_y equal to 19 m. Plots denoted by (a) and (b) are related to r equal to 7 m and 12 m, respectively. Plots denoted by (i), (ii), (iii) and (iv) are related to N equal to 7, 12, 15 and 21, respectively.
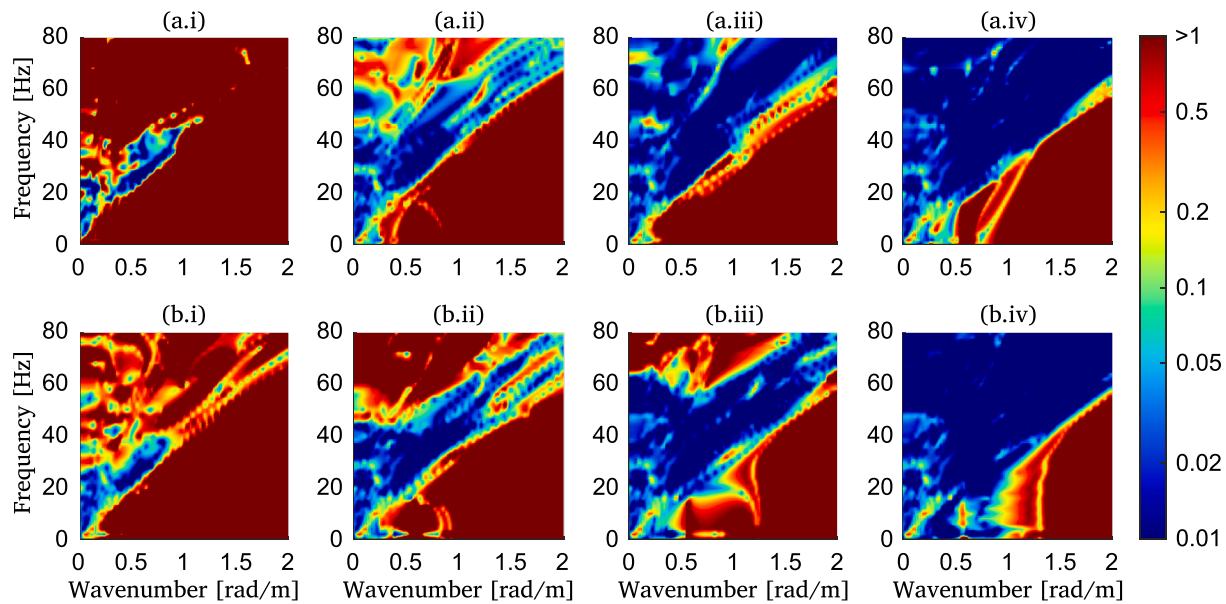
Fig. 18. Error ε for the parametric study performed in the context of Layered A case study and for L_z equal to 8 m and L_y equal to 30 m. Plots denoted by (a) and (b) are related to r equal to 7 m and 12 m, respectively. Plots denoted by (i), (ii), (iii) and (iv) are related to N equal to 7, 12, 15 and 21, respectively.

building vertical distance, the predominant layer in the propagation path can be considered instead of the upper for the application of the empirical rule. It is also found that small distances between the virtual sources set and the building structure could compromise the accuracy of the method. Particularly, it is found that distances below one half S-wave wavelength should be avoided, since they lead to numerical instabilities of the method. Finally, the proposed method is found to be insignificantly affected by the building-tunnel dynamic coupling for building-tunnel distances above 20 m. Regarding the collocation points distribution, an equispaced distribution of sensors along the surface at which the building structure will be constructed is found to be suitable. Although these guidelines for the design of virtual sources and collocation points distributions to properly apply the proposed hybrid methodology are derived from to 2D and 2.5D examples, the 3D nature of the 2.5D domain leads to the conclusion that these guidelines are also valid for fully 3D problems.

The proposed hybrid model simplifies the usual numerical prediction approach commonly adopted to deal with detailed assessment studies, since a model of the railway infrastructure is no longer required. Moreover, it reduces the uncertainty of the prediction due to the use of experimental measurements of the particular site under consideration. In addition, it provides a higher accuracy and flexibility than empirical models based on experimental transmissibility functions between the soil surface and the building. This methodology could also be used for the prediction of re-radiated noise inside buildings if a noise radiation model in cavities is considered [44–46]. More research should be conducted to fully define the experimental implementation of the present methodology in real cases, although conclusions of this work can serve as preliminary general guidelines on this regard. Furthermore, the methodology can be also used in the context of a fully numerical model in order to weakly couple a model of a building structure based on shallow or deep foundations with a model of a track-tunnel-soil system.

Authors statement

Robert Arcos: Conceptualization, Methodology, Software, Writing – review & editing, Visualization. Paulo J. Soares: Software, Investigation, Visualization, Writing – review & editing. Pedro Alves Costa: Writing – review & editing, Project administration, Funding acquisition. Luís Godinho: Writing – review & editing, Funding acquisition.

Declaration of competing interest

The authors declare that they have no known competing financial interests or personal relationships that could have appeared to influence the work reported in this paper.

Acknowledgements

References

[1] Balendra T, Chua KH, Lo KW, Lee SL. Steady-state vibration of subway-soil-building system. J Eng Mech 1989;115:145–62.
[2] Balendra T, Koh CG, Ho YC. Dynamic response of buildings due to trains in underground tunnels. Earthq Eng Struct Dynam 1991;20:275–91.
[3] Trochides A. Ground-borne vibrations in buildings near subways. Appl Acoust 1991;32:289–96.
[4] Sheng X, Jones CJC, Thompson DJ. Prediction of ground vibration from trains using the wavenumber finite and boundary element methods. J Sound Vib 2006;293:575–86.
[5] Fiala P, Degrande G, Augusztinovicz F. Numerical modelling of ground-borne noise and vibration in buildings due to surface rail traffic. J Sound Vib 2007;301:718–38.

[6] Lombaert G, Degrande G, Clouteau D. Numerical modelling of free field traffic-induced vibrations. Soil Dynam Earthq Eng 2000;19:473–88.

[7] Lopes P, Costa PA, Ferraz M, Calçada R, Cardoso AS. Numerical modeling of vibrations induced by railway traffic in tunnels: from the source to the nearby buildings. Soil Dynam Earthq Eng 2014;61–62:269–85.

[8] Lopes P, Ruiz JF, Alves Costa P, Medina Rodríguez L, Cardoso AS. Vibrations inside buildings due to subway railway traffic. Experimental validation of a comprehensive prediction model. Sci Total Environ 2016;568:1333–43.

[9] Hussein M, Hunt H, Kuo K, Alves Costa P, Barbosa J. The use of sub-modelling technique to calculate vibration in buildings from underground railways. Proc Inst Mech Eng - Part F J Rail Rapid Transit 2013;229:303–14.

[10] Quagliata A, Ahearn M, Boeker E, Roof C, Volpe JA. Transit noise and vibration impact assessment manual, technical report 0123. Federal Transit Administration; 2018.

[11] Sadeghi J, Esmaeili MH, Akbari M. Reliability of FTA general vibration assessment model in prediction of subway induced ground borne vibrations. Soil Dynam Earthq Eng 2019;117:300–11.

[12] International Organization for Standardization. ISO 14837-1. Mechanical vibration. In: Ground-borne noise and vibration arising from rail systems, vol. 1. General Guidance; 2005.

[13] Lurcock DEJ, Thompson DJ, Bewes OG. Attenuation of railway noise and vibration in two concrete frame multi-storey buildings, noise and vibration mitigation for rail transportation systems. 2015. p. 511–8.

[14] Anderson D, Shimada S, Hanson D. 1dB per floor? How does noise and vibration propagate in high-rise buildings near railway lines? In: Degrande G, Lombaert G, Anderson D, de Vos P, Gautier P-E, Iida M, Nelson JT, Nielsen JCO, Thompson DJ, Tielkes T, Towers DA, editors, editors. Proceedings of the 13th International Workshop on Railway Noise, 16-19 September 2019, Ghent, BelgiumGhent, volume 150 of Notes on Numerical Fluid Mechanics and Multidisciplinary Design, 150. Springer Nature Switzerland AG; 2021. p. 496–503.

[15] Kuo KA, Papadopoulos M, Lombaert G, Degrande G. The coupling loss of a building subject to railway induced vibrations: numerical modelling and experimental measurements. J Sound Vib 2019;442:459–81.

[16] Madshus C, Beassason B, Hårvik L. Prediction model for low frequency vibration from high speed railways on soft grounds. J Sound Vib 1996;193:195–203.

[17] Kuppelwieser H, Ziegler A. A tool for predicting vibration and structure-borne noise immissions caused by railways. J Sound Vib 1996;193:261–7.

[18] Lombaert G, Degrande G, Clouteau D. The influence of the soil stratification on free field traffic-induced vibrations. Arch Appl Mech 2001;71:661–78.

[19] Schevenels M, Lombaert G, Degrande G, François S. A probabilistic assessment of resolution in the SASW test and its impact on the prediction of ground vibrations. Geophys J Int 2008;172:262–75.

[20] Jones S, Kuo K, Hussein M, Hunt H. Prediction uncertainties and inaccuracies resulting from common assumptions in modelling vibration from underground railways. Proc Inst Mech Eng - Part F J Rail Rapid Transit 2012;226:501–12.

[21] Arnst M, Clouteau D, Chebli H, Othman R, Degrande G. A non-parametric probabilistic model for ground-borne vibrations in buildings. Probabilist Eng Mech 2006;21:18–34.

[22] Schevenels M. The impact of uncertain dynamic soil characteristics on the prediction of ground vibration. Ph.D. thesis. Katholieke Universiteit Leuven; 2007.

[23] Lopes P, Alves Costa P, Calçada R, Silva Cardoso A. Influence of soil stiffness on building vibrations due to railway traffic in tunnels: numerical study. Comput Geotech 2014;61:277–91.

[24] Papadopoulos M, François S, Degrande G, Lombaert G. The influence of uncertain local subsoil conditions on the response of buildings to ground vibration. J Sound Vib 2018;418:200–20.

[25] Papadopoulos M, Kuo K, Germonpré M, Verachtert R, Zhang J, Maes K, Lombaert GG Degrande. Numerical prediction and experimental validation of railway induced vibration in a multi-storey office building. In: Degrande G, Lombaert G, Anderson D, de Vos P, Gautier P-E, Iida M, Nelson JT, Nielsen JCO, Thompson DJ, Tielkes T, Towers DA, editors, editors. Proceedings of the 13th International Workshop on Railway Noise, 16-19 September 2019, Ghent, BelgiumGhent, volume 150 of Notes on Numerical Fluid Mechanics and Multidisciplinary Design,, 150. Springer Nature Switzerland AG; 2021. p. 529–37.

[26] Kuo KA, Verbraken H, Degrande G, Lombaert G. Hybrid predictions of railway induced ground vibration using a combination of experimental measurements and numerical modelling. J Sound Vib 2016;373:263–84.

[27] Auersch L. Building response due to ground vibration - simple prediction model based on experience with detailed models and measurements. Int J Acoust Vib 2010;15:101–12.

[28] Sanayei M, Kayiparambil P A, Moore JA, Brett CR. Measurement and prediction of train-induced vibrations in a full-scale building. Eng Struct 2014;77:119–28.

[29] López-Mendoza D, Romero A, Connolly DP, Galvín P. Scoping assessment of building vibration induced by railway traffic. Soil Dynam Earthq Eng 2017;93: 147–61.

[30] López-Mendoza D, Connolly DP, Romero A, Kouroussis G, Galvín P. A transfer function method to predict building vibration and its application to railway defects. Construct Build Mater 2020;232.

[31] Coulier P, Lombaert G, Degrande G. The influence of source-receiver interaction on the numerical prediction of railway induced vibrations. J Sound Vib 2014;333: 2520–38.

[32] Fairweather G, Karageorghis A, Martin PA. The method of fundamental solutions for scattering and radiation problems. Eng Anal Bound Elem 2003;27:759–69.

[33] Tadeu A, António J, Godinho L. Defining an accurate MFS solution for 2.5D acoustic and elastic wave propagation. Eng Anal Bound Elem 2009;33:1383–95.

[34] Amado-Mendes P, Alves Costa P, Godinho LM, Lopes P. 2.5D MFS-FEM model for the prediction of vibrations due to underground railway traffic. Eng Struct 2015; 104:141–54.

[35] R. Arcos, A. Clot, J. Romeu, Dynamic representation of excitation sources on construction- induced vibration problems based on multiple harmonic loads applied on the ground, in: Proceedings of 46th international congress and exposition on noise control engineering, [Hong-Kong].

[36] Hussein M, François S, Schevenels M, Hunt H, Talbot J, Degrande G. The fictitious force method for efficient calculation of vibration from a tunnel embedded in a multi-layered half-space. J Sound Vib 2014;333:6996–7018.

[37] Godinho L, Mendes PA, Tadeu A, Cadena-Isaza A, Smerzini C, Sanchez-Sesma FJ, Madec R, Komatitsch D. Numerical simulation of ground rotations along 2D topographical profiles under the incidence of elastic plane waves. Bull Seismol Soc Am 2009;99:1147–61.

[38] Coulier P, François S, Lombaert G, Degrande G. Coupled finite element – hierarchical boundary element methods for dynamic soil – structure interaction in the frequency domain. Int J Numer Methods Eng 2014;97:505–30.

[39] Hunt HEM. Prediction of vibration transmission from railways into buildings using models of infinite length. Veh Syst Dyn 1995;24:234–47.

[40] Clot A, Arcos R, Romeu J. Efficient three-dimensional building-soil model for the prediction of ground-borne vibrations in buildings. J Struct Eng - ASCE 2017;143: 1–13.

[41] Kausel E. Early history of soil-structure interaction. Soil Dynam Earthq Eng 2010; 30:822–32.

[42] Alves CJ. On the choice of source points in the method of fundamental solutions. Eng Anal Bound Elem 2009;33:1348–61.

[43] International Organization for Standardization. ISO 2631-2. Mechanical vibration and shock. Evaluation of human exposure to whole-body vibration. In: Part 2: vibration in buildings (1 Hz to 80 Hz); 2003.

[44] Colaço A, Alves Costa P, Amado-Mendes P, Godinho L. Prediction of vibrations and reradiated noise due to railway traffic: a comprehensive hybrid model based on a finite element method and method of fundamental solutions approach. J Vib Acoust 2017;139:061009.

[45] Ghangale D, Colaço A, Alves Costa P, Arcos R. A methodology based on structural finite element method-boundary element method and acoustic boundary element method models in 2.5D for the prediction of reradiated noise in railway-induced ground-borne vibration problems. J Vib Acoust 2019;141:031011.

[46] Costa PA, Arcos R, Soares P, Colaço A. Hybrid approach for the assessment of vibrations and re-radiated noise in buildings due to railway traffic: concept and preliminary validation. In: Advances in engineering materials, structures and systems: innovations, mechanics and applications - proceedings of the 7th international conference on structural engineering. Mechanics and Computation; 2019. p. 79–84. 2019.